INTERNATIONAL JOURNAL OF HYDROGEN ENERGY 36 (2011) 2471–2477

Available at www.sciencedirect.com

ScienceDirect

journal homepage: www.elsevier.com/locate/he

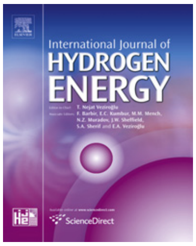

Environmental exposure of $2LiBH_4+MgH_2$ using empirical and theoretical thermodynamics

C.W. James Jr., D.A. Tamburello, K.S. Brinkman, J.R. Gray, B.J. Hardy, D.L. Anton*

Savannah River National Laboratory, Aiken, SC 29808, USA

ARTICLE INFO

Article history:
Received 20 January 2010
Received in revised form
5 May 2010
Accepted 6 May 2010
Available online 17 July 2010

Keywords:
Hydrogen storage
Environmental reactivity
Lithium borohydride
Magnesium hydride
Calorimetry

ABSTRACT

It has been shown that the consequence of environmental exposure can be qualitatively predicted by modeling the heat generated as a result of environmental exposure of reactive hydrides along with heat loss associated with conduction and convection with the ambient surroundings. To this end, an idealized finite volume model was developed to represent the behavior of dispersed hydride from a breached system. Semi-empirical thermodynamic calculations and substantiating calorimetric experiments were performed in order to quantify the energy released, energy release rates and to quantify the reaction products resulting from water and air exposure of a lithium borohydride and magnesium hydride combination. The hydrides, $LiBH_4$ and MgH_2, were studied in a 2:1 "destabilized" mixture which has been demonstrated to be reversible. Liquid water hydrolysis reactions were performed in a Calvet calorimeter equipped with a mixing cell using pH-neutral water. Water vapor and gaseous oxygen reactivity measurements were performed at varying relative humidities and temperatures by modifying the calorimeter and utilizing a gas circulating flow cell apparatus. The results of these calorimetric measurements were used to develop quantitative kinetic expressions for hydrolysis and air oxidation in these systems. Thermodynamic parameters obtained from these tests were then incorporated into a computational fluid dynamics model to predict both the hydrogen generation rates and concentrations along with localized temperature distributions. The results of these numerical simulations can be used to predict ignition events and the resultant conclusions will be discussed.

1. Introduction

An extensive study on the safe handling and properties of hydrogen gas released in air has been previously published by Fischer [1]. It was concluded that the most probable risks were associated with possible hydrogen gas release, ignition, and/or combustion. For hydrogen to be used in vehicular applications, high volumetric densities must be maintained to insure the utility of the vehicle is not compromised. To achieve these high volumetric densities, hydrogen storage in condensed chemical forms are being investigated. While the risks of using hydrogen gas are reasonably well understood, the risk of storing and using hydrogen in chemically condensed forms has not been thoroughly evaluated. A number of recent publications have begun to explore the risks of environmental exposure of these materials [2–5]. Either liquid or gaseous water contact has been identified as leading to the most vigorous reactions with complex hydrides generally speaking. This study will investigate, in depth, one specific candidate hydride, "destabilized" $2LiBH_4$:MgH_2, both empirically and

---

* *Corresponding author*. Tel.: +1 803 507 8551; fax: +1 803 652 8137.
E-mail address: donald.anton@srnl.doe.gov (D.L. Anton).

0360-3199/$ – see front matter © 2010 Professor T. Nejat Veziroglu. Published by Elsevier Ltd. All rights reserved.
doi:10.1016/j.ijhydene.2010.05.025

through three dimensional heat flow analyses. The "destabilized" mixture has been reported to have a >10 wt% H_2 capacity and rechargeable under reasonable pressure and temperature (1–10 atm and 20–100 °C) [6,7].

Environmental exposure studies of candidate storage materials are needed to quantify the reaction pathway, products and the quantity of heat released after a possible storage tank rupture or release scenarios. For example, the hydrolysis of lithium borohydride reacts with water as follows:

$$LiBH_4 + 2H_2O(\ell) \rightarrow LiBO_2 + 4H_2(g) \quad (1)$$

The hydrogen producing reaction, Equation (1), is an exothermic reaction with an enthalpy of 65.25 kJ/mol H_2. The heat released from this reaction may be combined with the released hydrogen and, along with oxygen present in the surrounding air, could provide the necessary conditions for ignition. The risks of this occurring depends on the kinetics of the reaction, the heat liberated through reaction, the concentration of the reactants and their spatial distribution, ambient conditions, balanced against heat loss through radiation, conduction and convection. Therefore, it is important to understand and quantify the potential risk of ignition resulting from accidental environmental exposure of condensed phase hydrogen storage materials under differing environmental exposure scenarios. This paper describes a modeling and experimental study with the aim of predicting consequences of the accidental release of $2LiBH_4 + MgH_2$ from hydrogen storage systems. The methodology and results developed in this work are directly applicable to any solid hydride material and/or accident scenario using appropriate boundary conditions and empirical data.

2. Experimental details

2.1. Calorimetry

To quantify the heat released through contact with dry and humidified air and liquid water, oxidation and hydrolysis studies were performed in a Calvet calorimeter. The heat flow (mW) was normalized with respect to hydride and plotted versus time. Liquid water tests were performed using a mixing cell with pH-neutral water to react 5–10 mg of solid with 1 ml of water. Controlled humidity air reaction measurements were conducted at varying relative humidity levels (30 and 60% RH) and temperatures (40 and 70 °C). For these measurements, the calorimeter equipped with a flow cell utilizing either argon or air as the carrier gas with a flow rate of 10 ml/min reacting with 5–10 mg of solid. Specimens were prepared by mixing commercially pure MgH_2 and $LiBH_4$ purchased from Aldrich Inc. Milling was conducted in a Spex mill for 1 h, under an argon atmosphere with a ball-to-sample ratio of 20:3.

2.2. Numerical modeling

The modeling effort has focused on incorporating chemical reaction rate data into the Navier–Stokes and energy conservation equations to create realistic simulations of heat and mass flow from hydrogen. The environmental scenario is described as a suspended sphere of materials with variable radius having a specified porosity. The radially symmetrical geometry was utilized to determine the critical pellet radius above which would lead to a potential reaction event. This geometry also minimized computational intensity by ignoring ground contact effects. Fig. 1 provides the basic model schematic. The governing equations solved for each analysis include mass, momentum, and energy balances, plus additional kinetics equations based on the calorimetry data at 70 °C for loosely-packed $2LiBH_4:MgH_2$ in contact with liquid water. This is a worst case scenario at the given environmental conditions. The thermal data was divided into four time segments, with each segment fit to a 4th-order polynomial. Table 1 lists the model parameters and constants for these models [8,9]. The following assumptions were made to simplify the analysis.

- The ambient fluid is dry air.
- The calorimetry data at 70 °C for the liquid water and $2LiBH_4:MgH_2$ is assumed to be the worst case scenario with the fast reaction rate and highest heat of reaction for this system.
- The heat and mass generation source is based upon the worst case scenario as stated in the assumption above and is modeled as temperature, pressure, and material composition independent. Thus, the heat and mass generation source, which varies with time and position, will continue regardless of the fluid or material temperature, fluid pressure, or species concentrations.
- All reactions begin in the outer shell of the hydride sphere.
- The material is a uniform 50% porous sphere.
- Mass transport considerations and limitations within the porous sphere that would be present due to binders or other pelletization considerations are not addressed in this work.

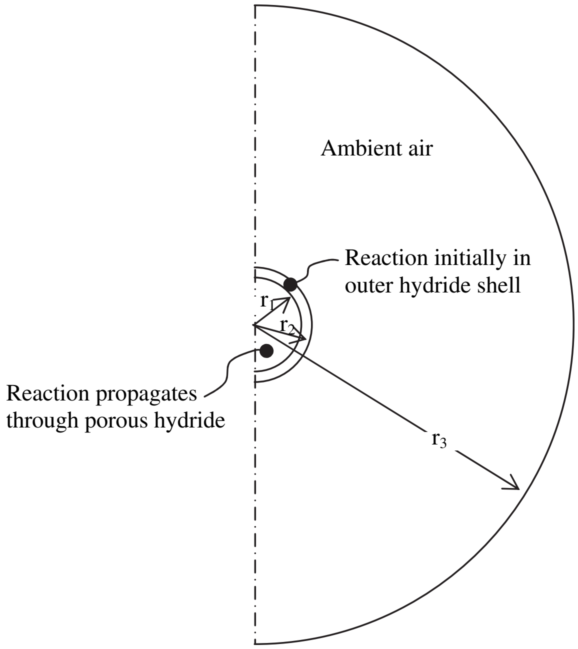

Fig. 1 – Axisymmetric sphere model schematic.

Table 1 – Model parameters for porous $2Li(BH_4):MgH_2$.

Parameter	Value			
Material porosity (ε)	0.5			
Particle diameter (D_p)	3.7×10^{-6} m			
Material density (ρ)	927 kg/m^3			
Material thermal conductivity (k)	0.5 W/m K			
Material specific heat (C_p)	1583 J/kg K			
Heat/mass generation	Based on calorimetry data			
Reaction propagation	0.03 mm/s[a]			
Model dimensions:	Model	r_1 (in)	r_2 (in)	r_3 (in)
	0.05 in	0.00	0.05	10.05
	¼ in	0.20	0.25	10.25
	½ in	0.45	0.50	10.50
	1 in	0.95	1.00	11.00
	1½ in	1.45	1.50	11.50
	2 in	1.95	2.00	12.00
	2½ in	2.45	2.50	12.50

a Based on contamination model [9].

- The material properties are constant during the simulation.
- The ambient air properties are allowed to change with temperature and pressure via the ideal gas law.
- The built-in hydrogen–air reaction within FLUENT [10] is used to mark the hydrogen ignition even when/if it occurs. However, the model is only designed to capture the events leading up to the ignition event and is not designed to model the ignition event itself or the events following the ignition event.

3. Results and discussion

3.1. *Liquid water calorimetry*

Fig. 2a gives a typical calorimetric result of heat flow versus time for liquid water hydrolysis of $2LiBH_4+MgH_2$ at 40 and 70 °C. As displayed in Fig. 2a, a temperature increase of 30 °C (from 40 to 70 °C) resulted in a modified calorimetric signal. Both the total heat released for the hydrolysis reaction was different at the two temperatures as well as the final crystalline phase composition suggesting different reaction pathways occurred. Amorphous lithium products were observed at the lower 40 °C temperature along with $Mg(OH)_2$, while crystalline lithium compounds such as $Li(H_2O)_4B(OH)_4(H_2O)_2$ were observed in the higher temperature hydrolysis reaction at 70 °C. The integrated area under the heat flow signal at time *t* in Fig. 2a divided by the total reaction enthalpy (total area under the heat flow signal) was used to estimate the reaction progress in (percent) as displayed in Fig. 2b. The result allows us to quantify the increase in reaction rate: a temperature increase of 30 °C (from 40 to 70 °C) resulted in an increase of the reaction progress from 40 to 70% after 1 h.

3.2. *Water vapor calorimetry*

3.2.1. *Air versus argon carrier gas*

The effects of water vapor in air versus water vapor in an argon carrier gas were studied to separate the effects of hydrogen oxidation with air from gas phase water hydrolysis. Fig. 3 displays the heat flow signal from $LiBH_4$ reacted with water vapor (30% relative humidity) at 40 °C using air and argon as a carrier gas flowing at 10 ml/min. The energy release during the reactions were approximately the same for both cases: 30% RH air carrier gas 352 kJ/mol, 30% RH Argon carrier gas 340 kJ/mol, however the reaction in the presence of air reaches completion more quickly than in the presence of argon. XRD identified products were: air carrier gas ($LiB(OH)_4$, $LiB(OH)_2(O_2)$, $H_6B_2O_6$ and residual $LiBH_4$); argon carrier gas ($LiB(OH)_4$) illustrating different reactions occurred in the presence of oxygen. These results do not indicate oxidation of hydrogen after its release from the sample through hydration. This oxidation event would have resulted in a significantly increased heat of reaction.

3.2.2. *Relative humidity effects*

The heat flow signal was measured during humid air exposure for the mixture $2LiBH_4:MgH_2$ at 40 °C with both 30% RH and 60% RH. Fig. 4 displays the multiple heat releasing events that were observed in these experiments. The total amount of heat released was approximately the same at different relative humidity levels, with a value of 268 kJ/mol at 40 °C 30% RH and 251 kJ/mol at 40 °C 60% RH. The XRD results indicate $LiB(OH)_4$ and residual MgH_2 crystalline products for both levels of

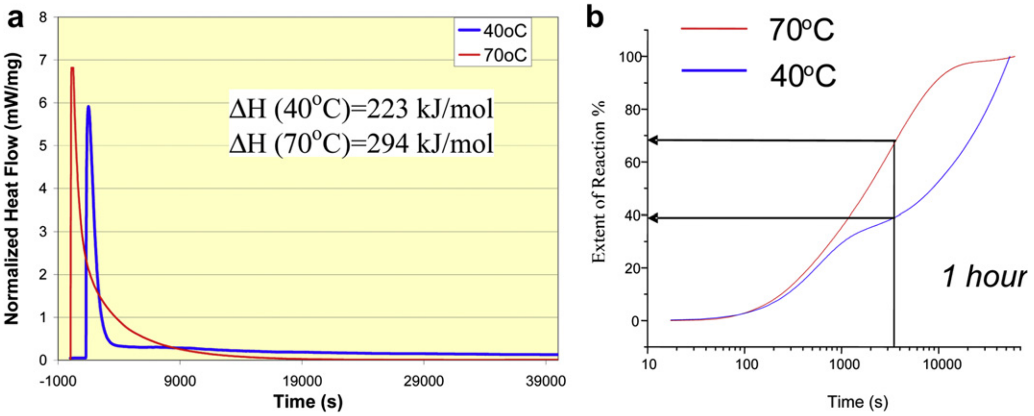

Fig. 2 – a) Heat flow from neutral water hydrolysis of $2LiBH_4:MgH_2$ at 40 °C and 70 °C and b) the reaction progress as a function of time determined from the integrated calorimetric signal.

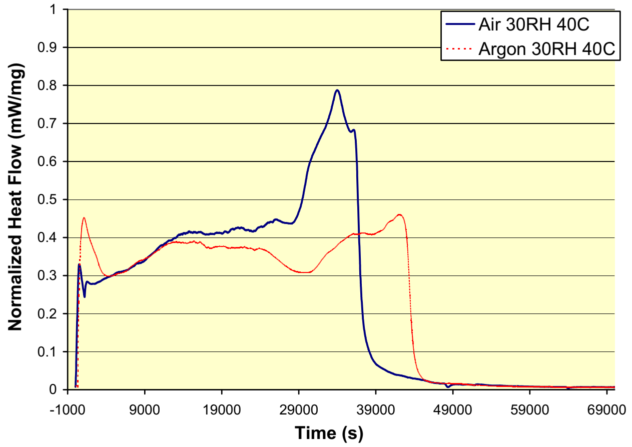

Fig. 3 – Normalized heat flow from $LiBH_4$ reacted with 30% relative humidity using air and argon as a carrier gas at 40 °C.

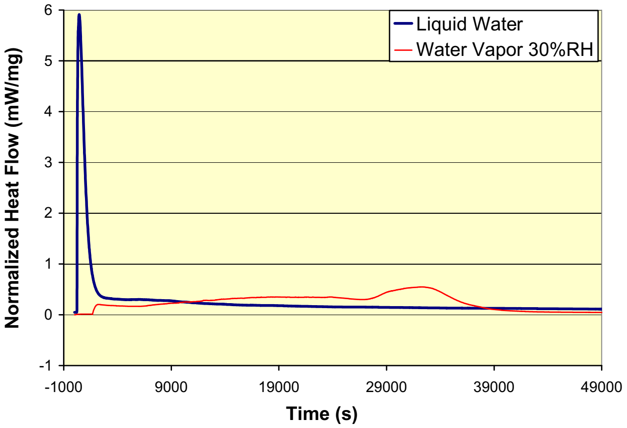

Fig. 5 – Normalized heat flow (mW/mg) during hydrolysis/oxidation of $2LiBH_4$:MgH_2 with liquid water at 40 °C and with 30% relative humidity air at 40 °C (10 ml/min flow rate).

relative humidity. In gas phase hydrolysis, the amount of water vapor seems only to impact the reaction time and not the pathway or final products. An increase in water vapor available for hydrolysis decreases the time required to complete the reaction. The reaction of $2LiBH_4$:MgH_2 with air at 70 °C and 30% relative humidity were performed, resulting in approximately the same crystalline products ($LiB(OH)_4$, and MgH_2) and total heat release (242 kJ/mol) as the reaction at 40 °C at varying relative humidity levels. The only impact of increased temperature seems to be an increase in the amount of water vapor in the air, thus speeding up the hydrolysis reaction.

3.3. *Water vapor versus liquid calorimetry*

Due to experimental constraints such as the geometry and pressure rating of the sample cells, and the type of experiment being conducted (gas or liquid contact), there is a range in the amount of water supplied to the starting material as a function of time. In a liquid water mixing experiment, an excess of 32 times the stoichiometric amount of water is added which remains constant during the duration of the experiment. In contrast, the amount of water added during gas flow experiments is determined by the flow rate, the gas and reaction temperature and thermodynamics of the water liquid/vapor equilibrium expressed through the relative humidity indicator. Since water vapor is added in a flow through configuration, the quantity provided for the hydrolysis reaction increases linearly with time. The saturation vapor pressure of water increases with temperature so that higher temperatures and higher relative humidity levels increase the amount of water available for the hydrolysis reaction.

Fig. 5 displays the normalized heat flow (mW/mg) for the $2LiBH_4$:MgH_2 reaction with liquid water in a mixing cell compared with water vapor in a gas flow cell. The amount of total water addition in excess of stoichiometry is 32 times for liquid water and 4 times (after a reaction time of 12 h) for the conditions of 40 °C and 30% relative humidity. The qualitative difference observed by heat flow is believed to be due to the difference in gas/solid versus liquid/solid interfacial reactions and is currently under further investigation. The total energy release of the water vapor reaction was greater (−268 kJ/mol) than the energy release upon liquid water hydrolysis (−223 kJ/mol). In addition the final crystalline reaction products were different in the two cases: the reaction with 30% relative humidity air resulted in $LiB(OH)_4$ and residual MgH_2, while the

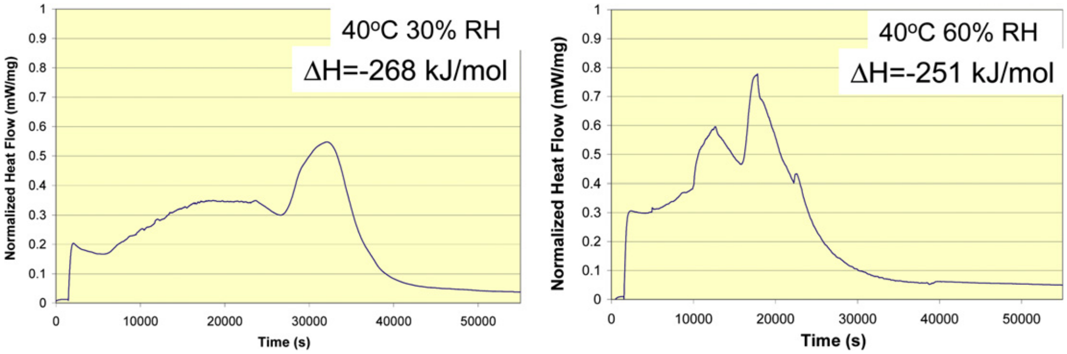

Fig. 4 – Normalized heat flow (mW/mg) for $2LiBH_4$:MgH_2 reacted with a) air at 40 °C and 30% relative humidity and b) air at 40 °C and 60% relative humidity.

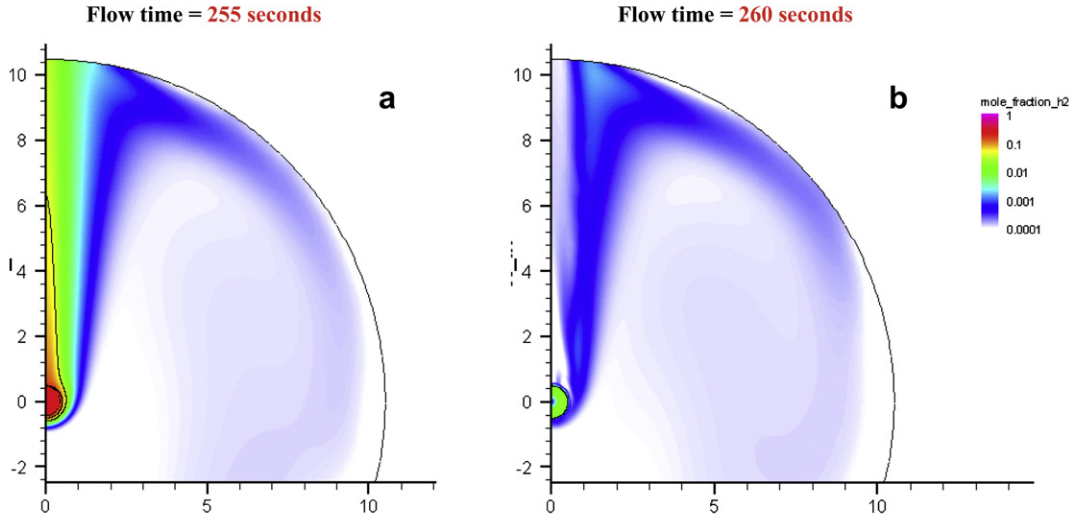

Fig. 6 – Mole fraction of H_2 before (a) and after (b) the hydrogen ignition for the axisymmetric sphere with a ½ inch radius.

liquid water hydrolysis resulted in $LiB(OH)_4$, $H_6B_2O_6$ and $LiB(OH)_2(O_2)$ phases along with amorphous components. Overall, in both the liquid mixing and gas flow reactions the trend is for a lower measured energy compared to the thermodynamically predicted reactions. A corollary to this is that the actual observed products do not match those predicted from thermodynamics and often have a significant degree of amorphous character. However, despite discrepancies in theoretical versus experimental thermodynamic properties, the kinetics of energy release empirically determined for these materials via calorimetry are of prime importance for modeling the environmental reactivity under accident scenarios as described in the subsequent section.

3.4. *Numerical modeling results*

Two sets of initial conditions were used to evaluate different scenarios. For the first, the hydride is initialized with ambient air filling the porous media. These scenarios assume that the hydride has been released from its container for a short amount of time prior to any chemical reaction occurring, which allows all of the hydrogen gas to evacuate from the hydride prior to the reaction and be replaced with ambient air. Results from these simulations are shown in Figs. 6 and 7 and summarized in Table 2. The smallest diameter hydride spheres (0.05 inch and ¼ inch models) never reach the lower flammability limit (LFL = 0.04) for hydrogen concentration,

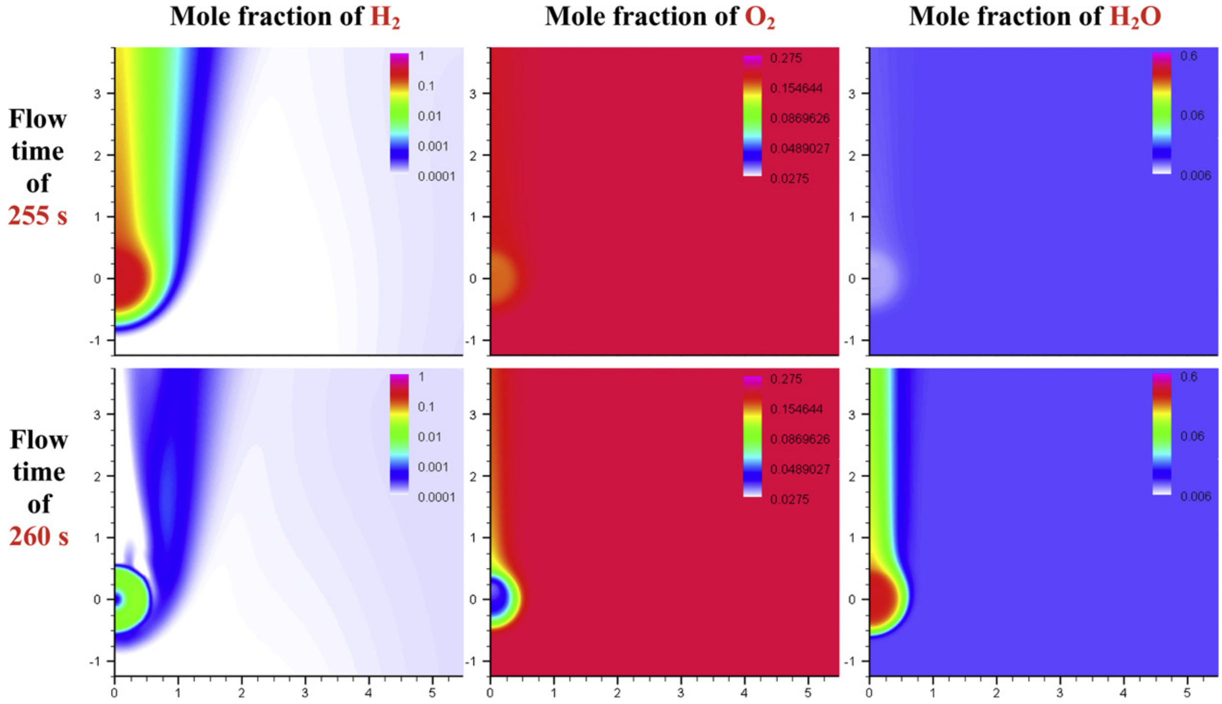

Fig. 7 – Mole fractions of H_2, O_2, and H_2O before and after hydrogen ignition (255 s and 260 s, respectively) for the axisymmetric sphere with a ½ inch radius.

Table 2 – Axisymmetric sphere results for air-initialized hydride.

Model	H_2 ignition event	H_2 mole fraction (mf)	Temperature
0.05 in	None	Maximum value of 0.0123 at $t = 160$ s	Maximum temperature of 164.2 °C at $t = 300$ s
0.25 in	None	LFL reached between $t = 55$ s and 60 s Max of 0.135 at $t = 230$ s	Maximum temperature of 752.4 °C at $t = 370$ s
0.50 in	Between $t = 255$ s and 260 s H_2 mf = 0.266 Temp = 569 °C and 571 °C	LFL reached between $t = 30$ s and 35 s Max of 0.266 at $t = 255$ s	Maximum temperature of 1422 °C at $t = 540$ s
1.0 in	Between $t = 200$ s & 203 s H_2 mf = 0.323 Temp = 327 °C and 361 °C	LFL reached at $t = 25$ s Max of 0.323 at $t = 200$ s	Maximum temperature of 2184 °C at $t = 963$ s
1.5 in	Between $t = 180$ s and 185 s H_2 mf = 0.343 Temp = 263 °C and 316 °C	LFL reached between $t = 20$ s and 25 s Max of 0.343 at $t = 180$ s	Temperature reaches 2250 °C at $t = 1000$ s (and still rising)
2.0 in	Between $t = 170$ s and 175 s H_2 mf = 0.361 Temp = 234 °C and 293 °C	LFL reached between $t = 20$ s and 25 s Max of 0.361 at $t = 170$ s	Temperature reaches 2563 °C at $t = 1000$ s (and still rising)
2.5 in	Between $t = 180$ s and 183 s H_2 mf = 0.410 Temp = 255 °C and 668 °C	LFL reached between $t = 20$ s and 25 s Max of 0.410 at $t = 180$ s	Temperature reaches 2312 °C at $t = 1000$ s (and still rising)

which means no reaction event occurs. For the larger spheres (½ inch and higher models), the LFL and/or the auto-ignition temperature (500 °C or 571 °C depending on the H_2 concentration) of hydrogen is reached and a reaction event occurs. Thus, there is a critical radius between ¼ and ½ inch that indicates the minimum amount of material necessary for a hydrogen ignition event to occur given the assumptions listed above.

Fig. 6 highlights the H_2 concentrations before (Fig. 6a, time = 255 s) and after (Fig. 6b, time = 260 s) the hydrogen ignition event occurs for the ½ inch hydride sphere model. The H_2 concentration (26.6% mf) is well above the LFL prior to the reaction event and then drops off rapidly after the event (~1.5% mf). Fig. 7 shows the species concentration for the other components of the hydrogen–air reaction for the ½ inch sphere model. Note that as the H_2 and O_2 burn away, water vapor (H_2O) increases in their place. Similar results are seen for the larger spheres (1 inch and greater models), but are not shown.

For the second scenario, the hydride is initialized with hydrogen gas filling the porous media. This scenario assume that the chemical reaction occurs immediately after the hydride is released from its container, which means the porous space within the hydride is still full of 100% hydrogen gas at the start of the numerical simulation. It was observed that due to the high dissipation rate of H_2 into the ambient atmosphere, most of the hydrogen has been expelled from the hydride prior to the start of the chemical reaction (mass/heat generation) within the simulation. Thus, the hydrogen-initialized hydride models yielded similar results to the air-initialized hydride models and are not shown.

4. Conclusions

The heat flow of destabilized $2LiBH_4{:}MgH_2$ system was measured under different conditions that represented various environmental exposure conditions (dry, humid, and wet). The total heat released and the final crystalline products were different for the hydrolysis reaction at 40 °C and 70 °C. Amorphous lithium products were observed at the lower 40 °C temperature, while crystalline lithium compounds were observed at 70 °C. In the gas phase reaction, the presence of water vapor increased the reaction time, but does not change the final product. However, the larger heat flow in the presence of liquid water versus water vapor could be attributed to the gas/solid versus liquid/solid interfacial reactions Given the numerical simulation assumptions, there is a definitive amount of material (i.e. critical radius of $0.25'' < r < 0.50''$) needed for a hydrogen reaction event to occur. When the spherical radius is smaller than this critical radius, hydrogen is released to the ambient without a reaction event. When larger amounts of hydride are present (i.e. the spherical radius is larger than the critical radius), enough heat and hydrogen are evolved simultaneously so that an ignition event is possible.

Acknowledgements

The authors would like to thank David Missimer and Joseph Wheeler for their XRD and laboratory support, respectively. This work was funded under the U.S. Department of Energy (DOE) hydrogen storage testing, safety, and analysis program managed by Dr. Ned Stetson.

REFERENCES

[1] Fischer M. Safety aspects of hydrogen combustion in hydrogen energy-systems. Int J Hydrogen Energy 1986;11: 593–601.

[2] Brinkman K, Gray J, Hardy B, Anton D. The hydrolysis and oxidation behavior of lithium borohydride and magnesium hydride determined by calorimetry. In: Proceedings of the

Materials Research Society (MRS), 2008 Spring Meeting. San Francisco, California HH-0314.
[3] Mosher DA, Arsenault S, Tang X, Anton DL. Design, fabrication and testing of $NaAlH_4$ based hydrogen storage systems. J Alloys Compd 2007;446–447:707–12.
[4] Lohstroh W, Fichtner M, Breitung W. Complex hydrides as solid storage materials: first safety tests. Int J Hydrogen Energy 2009; 34:5981–5.
[5] Tanaka H, Tokoyoda K, Matsumoto M, Suzuki Y, Kiyobayashi T, Kuriyama N. Hazard assessment of complex hydrides as hydrogen storage materials. Int J Hydrogen Energy 2009;34:3210–8.
[6] Satyapal S, Petrovic J, Read C, Thomas G, Ordaz G. The US Department of Energy's National Hydrogen Storage Project: progress towards meeting hydrogen-powered vehicle requirements. Catal Today 2007;120:246–56.
[7] Vajo JJ, Olson GL. Hydrogen storage in destabilized chemical systems. Scr Mater 2007;56:829–34.
[8] Hardy BJ. Integrated hydrogen storage system model. Report, WSRC-TR-2007-00440, rev. 0. Savannah River National Laboratory; November 16, 2007.
[9] Dedrick DE, Kanouff MP, Larson RS, Bradshaw RW, Graetz J, Hwang S. Predictions of solid-state hydrogen storage system contamination process. In: Proceedings of International Conference on Hydrogen Safety (ICHS). Corsica, France; 2009.
[10] FLUENT6. Fluent, Inc.; 2005.